

Effect of Mn-doping on performance of $\text{Li}_3\text{V}_2(\text{PO}_4)_3/\text{C}$ cathode material for lithium ion batteries

ZHAI Jing¹, ZHAO Min-shou^{1,2}, WANG Dan-dan¹

1. College of Environmental and Chemical Engineering, Yanshan University, Qinhuangdao 066004, China;
2. State Key Laboratory of Metastable Material Science and Technology, Yanshan University, Qinhuangdao 066004, China

Received 17 May 2010; accepted 8 October 2010

Abstract: $\text{Li}_3\text{V}_{2-2/3x}\text{Mn}_x(\text{PO}_4)_3$ ($0 \leq x \leq 0.12$) powders were synthesized by sol-gel method. The effect of Mn^{2+} -doping on the structure and electrochemical performances of $\text{Li}_3\text{V}_2(\text{PO}_4)_3/\text{C}$ was characterized by XRD, SEM, XPS, galvanostatic charge/discharge and electrochemical impedance spectroscopy (EIS). The XRD study shows that a small amount of Mn^{2+} -doped does not alter the structure of $\text{Li}_3\text{V}_2(\text{PO}_4)_3/\text{C}$ materials, and all Mn^{2+} -doped samples are of pure single phase with a monoclinic structure (space group $P2_1/n$). The XPS analysis indicates that valences state of V and Mn are +3 and +2 in $\text{Li}_3\text{V}_{1.94}\text{Mn}_{0.09}(\text{PO}_4)_3/\text{C}$, respectively, and the citric acid in raw materials was decomposed into carbon during calcination, and residual carbon exists in $\text{Li}_3\text{V}_{1.94}\text{Mn}_{0.09}(\text{PO}_4)_3/\text{C}$. The results of electrochemical measurements show that Mn^{2+} -doping can improve the cyclic stability and rate performance of these cathode materials. The $\text{Li}_3\text{V}_{1.94}\text{Mn}_{0.09}(\text{PO}_4)_3/\text{C}$ cathode material shows the best cyclic stability and rate performance. For example, at the discharge current density of 40 mA/g, after 100 cycles, the discharge capacity of $\text{Li}_3\text{V}_{1.94}\text{Mn}_{0.09}(\text{PO}_4)_3/\text{C}$ declines from initial 158.8 mA·h/g to 120.5 mA·h/g with a capacity retention of 75.9%; however, that of the Mn-undoped sample declines from 164.2 mA·h/g to 72.6 mA·h/g with a capacity retention of 44.2%. When the discharge current is increased up to 1C, the initial discharge capacity of $\text{Li}_3\text{V}_{1.94}\text{Mn}_{0.09}(\text{PO}_4)_3/\text{C}$ still reaches 146.4 mA·h/g, and the discharge capacity maintains at 107.5 mA·h/g after 100 cycles. The EIS measurement indicates that Mn^{2+} -doping with a appropriate amount of Mn^{2+} decreases the charge transfer resistance, which is favorable for the insertion/extraction of Li^+ .

Key words: lithium ion batteries; cathode materials; $\text{Li}_3\text{V}_2(\text{PO}_4)_3$; sol-gel; doping

1 Introduction

Since lithium iron phosphate, one kind of lithiated transition metal polyanion material based on PO_4^{3-} , was first reported as a cathode material for lithium-ion batteries by PADHI et al 1997[1], the framework materials based on the phosphate polyanion have been identified as potential electroactive materials for lithium-ion batteries, and $\text{Li}_3\text{V}_2(\text{PO}_4)_3$ is one of them. By comparing with the commercially used LiCoO_2 , LiNiO_2 , LiMn_2O_4 and their derivatives, $\text{Li}_3\text{V}_2(\text{PO}_4)_3$ cathode material has the outstanding advantages, such as stable framework, relatively high voltage, excellent heat stability, satisfactory safety and large theoretic capacity.

However, the main drawbacks of pristine $\text{Li}_3\text{V}_2(\text{PO}_4)_3$ are its very low intrinsic electronic conductivity and slow transport of Li ion, which results in poor cycling stability and rate performance. This

makes it difficult to utilize $\text{Li}_3\text{V}_2(\text{PO}_4)_3$ cathode material fully in lithium ion batteries[2–3]. To solve this problem, many efforts have been made to improve the performance of $\text{Li}_3\text{V}_2(\text{PO}_4)_3$ cathode material, including preparation of small radius and homogeneous particles[4–5], carbon coating[6–11] and metal cation doping[12–15]. The modification researches have improved the comprehensive electrochemical performance of $\text{Li}_3\text{V}_2(\text{PO}_4)_3$ to different extents. However, Mn-doping in $\text{Li}_3\text{V}_2(\text{PO}_4)_3/\text{C}$ has not been concerned in published papers yet. In this work, the effect of Mn-doping on the structure and electrochemical performance of $\text{Li}_3\text{V}_2(\text{PO}_4)_3/\text{C}$ was investigated.

2 Experimental

2.1 Preparation of $\text{Li}_3\text{V}_{2-2/3x}\text{Mn}_x(\text{PO}_4)_3$ ($0 \leq x \leq 0.12$)

$\text{Li}_3\text{V}_{2-2/3x}\text{Mn}_x(\text{PO}_4)_3/\text{C}$ ($x=0.03, 0.06, 0.09, 0.12$) cathode materials were synthesized by sol-gel method.

$V_2O_5 \cdot nH_2O$ hydro-gel was firstly prepared as follows: 10% (volume fraction) H_2O_2 solution was slowly added to V_2O_5 with vigorously stirring in ice-water until a clear orange solution formed, and then brownish homogeneous V_2O_5 gels were obtained after 4 h at 35 °C. Aqueous solution of the stoichiometric $NH_4H_2PO_4$, $CH_3COOLi \cdot 2H_2O$, $(CH_3COO)_2Mn \cdot 4H_2O$ and citric acid were added to the $V_2O_5 \cdot nH_2O$ hydro-gels, respectively. The mixture was heated with continuous stirring at 80 °C until the blue precursor was obtained. The obtained gel was dried in a vacuum oven at 80 °C, and then the powder sample was ground, pelletized and heated at 300 °C in a furnace with flowing nitrogen gas for 4 h; then temperature rose to 800 °C at a rate of 15 °C/min and kept for 5.5 h with a stream of nitrogen gas. The sample was taken out when the temperature was cooled down to room temperature, and then ground. The undoped $Li_3V_2(PO_4)_3/C$ sample was also prepared through the same method for comparison except without addition of $(CH_3COO)_2Mn \cdot 4H_2O$.

2.2 Sample characterization

X-ray diffraction pattern of the sample was carried out with 2θ between 10° and 60° by using a D/Max III diffractometer with Cu K_α radiation, at the scan speed of 2 (°)/min and voltage of 40 kV. The X-ray photoelectron spectroscopy (XPS) was obtained for the $Li_3V_{1.94}Mn_{0.09}(PO_4)_3/C$ sample by using Kratos Axis Ultra DLD spectrometer with monochromatic Al K_α radiation. The morphology of the sample was observed using the Hitachi S-4800 scanning electron microscope instrument (SEM).

2.3 Electrochemical tests

Electrochemical performances of the samples were evaluated in columned Li test cell. The cathode material was prepared by mixing the products with acetylene black and polyvinylidene fluoride (PVDF) binder at a mass ratio of 80:15:5 in *N*-methyl-2-pyrrolidone (NMP). The obtained slurry was coated on Al foil, dried under the infrared light and foursquare strips with dimensions of 8 mm×8 mm were cut into with active material of about 2 mg. After the strips were dried at 120 °C for 12 h in a vacuum, two-electrode electrochemical cell was assembled in a Mikrouna glove box filled with high-pure argon where the lithium metal foil was used as anode, Celgard® 2320 as separator and 1 mol/L $LiPF_6$ in EC:DMC (1:1, volume fraction) as electrolyte, then charge/discharge test was carried out using a Neware battery tester. The electrochemical measurements were performed in the voltage range of 3.0–4.8 V at room temperature. EIS measurements were carried out in three-electrode cell by using CHI 660A electrochemical analyzer (Chenhua, Shanghai, China) with ± 5 mV ac

signal and a frequency range of 10^5 – 10^{-2} Hz and 4.8 V.

3 Results and discussion

3.1 Sample characterization

XRD patterns of $Li_3V_{2-2/3x}Mn_x(PO_4)_3/C$ ($0 \leq x \leq 0.12$) are shown in Fig.1. It is obvious that all samples are of pure single phase with a monoclinic structure (space group $P2_1/n$), and the result is consistent with the published result[16]. No other phases are detected in the XRD patterns, indicating that Mn^{2+} ions are completely substituted into the crystal lattice of $Li_3V_2(PO_4)_3$, and a low dose of Mn^{2+} -doping does not alter the basic $Li_3V_2(PO_4)_3$ crystal structure. The amount of carbon in $Li_3V_2(PO_4)_3/C$ is about 4.4% in mass fraction measured by thermogravimetric analysis.

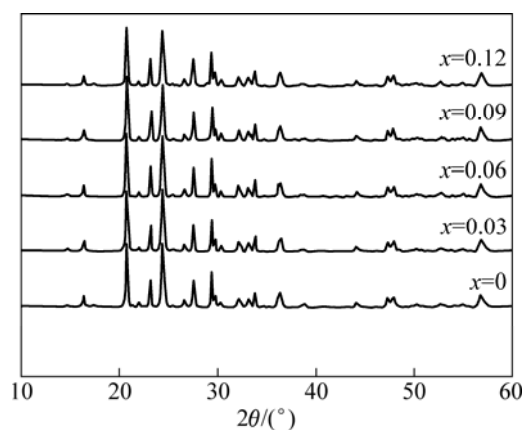


Fig.1 XRD patterns of $Li_3V_{2-2/3x}Mn_x(PO_4)_3/C$ ($0 \leq x \leq 0.12$)

The XPS spectra of V2p, Mn2p and C1s in the $Li_3V_{1.94}Mn_{0.09}(PO_4)_3/C$ sample are illustrated in Fig.2. Fig.2 shows that the V2p core level fits to a single peak with a binding energy of 517.2 eV, matching well with the reported result[15], so the oxidation state of V in $Li_3V_{1.94}Mn_{0.09}(PO_4)_3/C$ is +3. The Mn2p XPS also shows a single peak with a binding energy of 640.9 eV, similar to that observed in MnO (640.6 eV)[17], so the oxidation state of Mn in $Li_3V_{1.94}Mn_{0.09}(PO_4)_3/C$ is +2. The C1s XPS shows that the peak OC—O with a binding energy of 288.4 eV is absent, while the peak C—C with a binding energy of 284.6 eV occurs in the spectra of the $Li_3V_{1.94}Mn_{0.09}(PO_4)_3/C$. This indicates that citrate was decomposed into carbon during calcination, and residual carbon exists in $Li_3V_{1.94}Mn_{0.09}(PO_4)_3/C$. This is beneficial to enhance the electronic conductivity for $Li_3V_{1.94}Mn_{0.09}(PO_4)_3/C$.

The SEM images of the $Li_3V_{1.94}Mn_{0.09}(PO_4)_3/C$ and $Li_3V_2(PO_4)_3/C$ are presented in Fig.3. The particles of them show good crystallinity. The particles of the $Li_3V_2(PO_4)_3/C$ sample presents piece shape and are agglomerated with each other. The grains of

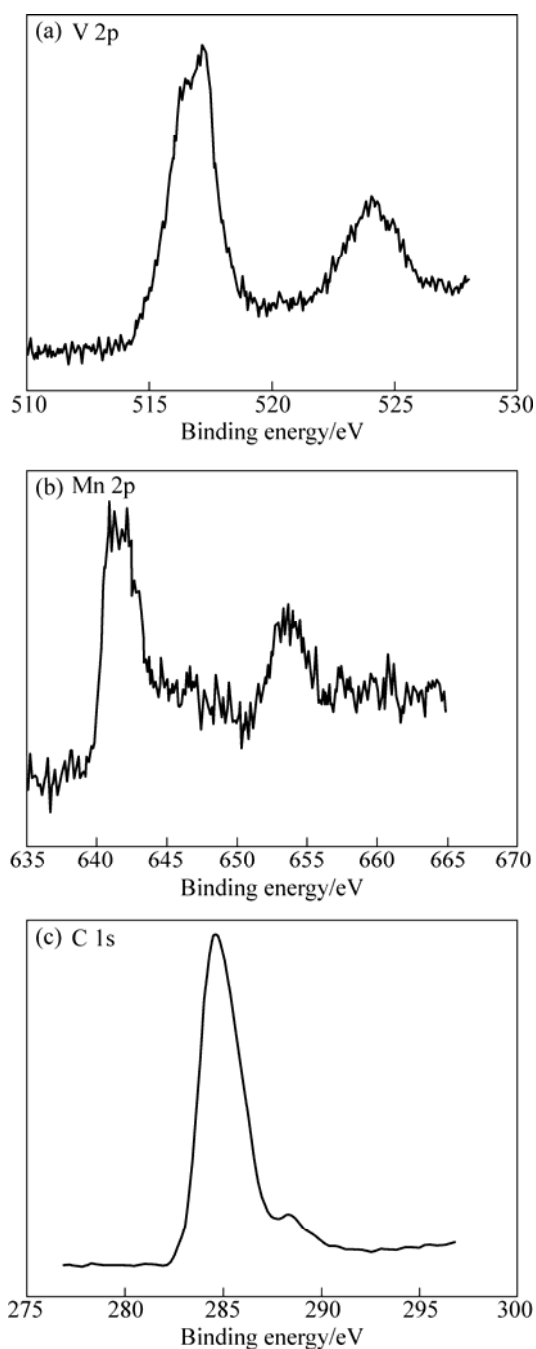


Fig.2 XPS spectra of V 2p (a), Mn 2p (b) and C 1s (c) in $\text{Li}_3\text{V}_{1.94}\text{Mn}_{0.09}(\text{PO}_4)_3/\text{C}$

$\text{Li}_3\text{V}_{1.94}\text{Mn}_{0.09}(\text{PO}_4)_3/\text{C}$ sample are like ball shape, and the particles are smaller and more homogeneous than $\text{Li}_3\text{V}_2(\text{PO}_4)_3/\text{C}$ sample.

3.2 Galvanostatic electrochemical measurements

The second charge/discharge curves are shown in Fig.4 for the $\text{Li}/\text{Li}_3\text{V}_{1.94}\text{Mn}_{0.09}(\text{PO}_4)_3$ and $\text{Li}/\text{Li}_3\text{V}_2(\text{PO}_4)_3$ test cells at 40 mA/g current density in the range of 3.0–4.8 V at room temperature. For $\text{Li}_3\text{V}_2(\text{PO}_4)_3/\text{C}$ sample, Fig.4(a) shows clearly four plateaus in the charge process and three plateaus in the discharge process,

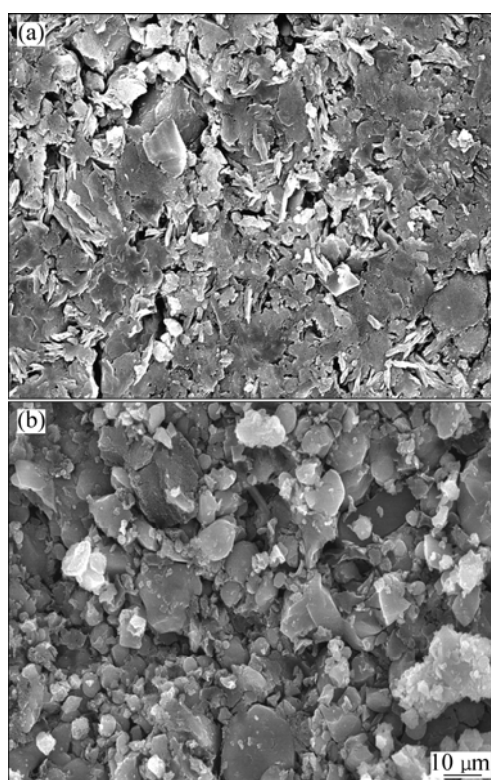


Fig.3 SEM images of $\text{Li}_3\text{V}_2(\text{PO}_4)_3/\text{C}$ (a) and $\text{Li}_3\text{V}_{1.94}\text{Mn}_{0.09}(\text{PO}_4)_3/\text{C}$ (b)

which have definite boundary. For $\text{Li}_3\text{V}_{1.94}\text{Mn}_{0.09}(\text{PO}_4)_3/\text{C}$ sample, there are four plateaus in the charge process and two plateaus in the discharge process. Compared with the $\text{Li}_3\text{V}_2(\text{PO}_4)_3/\text{C}$ sample, the first two discharge plateaus of $\text{Li}_3\text{V}_{1.94}\text{Mn}_{0.09}(\text{PO}_4)_3/\text{C}$ sample are merged into one. The result agrees with that of Ti-doped one[14]. Electrochemical reaction leading to multiphase reaction mechanism around plateaus usually presents new interphases, which decreases Li^+ transport and accordingly affects the electrochemical performance. The more complicated the phase transition is, the more difficult the transports of Li^+ is[18]. The conclusion may be drawn that there is a tendency from multiphase reaction to single-phase reaction in the charge-discharge processes by doping Mn to $\text{Li}_3\text{V}_2(\text{PO}_4)_3/\text{C}$. This change is beneficial to Li^+ insertion/extraction and reduces the variation of cell volume during cycling, which significantly improves the cycle stability, as confirmed in Fig.5.

Fig.5 shows cycling performance of $\text{Li}_3\text{V}_{2-2/3x}\text{Mn}_x(\text{PO}_4)_3$ ($x=0, 0.03, 0.06, 0.09, 0.12$) in the voltage range of 3.0–4.8 V at current density of 40 mA/g. It can be seen that the highest discharge capacity of Mn-doped samples is lower than that of undoped one; however, the cyclic stability is apparently improved except for the sample with Mn-doped 0.03 after 40 cycles, especially the cyclic stability of $\text{Li}_3\text{V}_{1.94}\text{Mn}_{0.09}(\text{PO}_4)_3/\text{C}$ is significantly

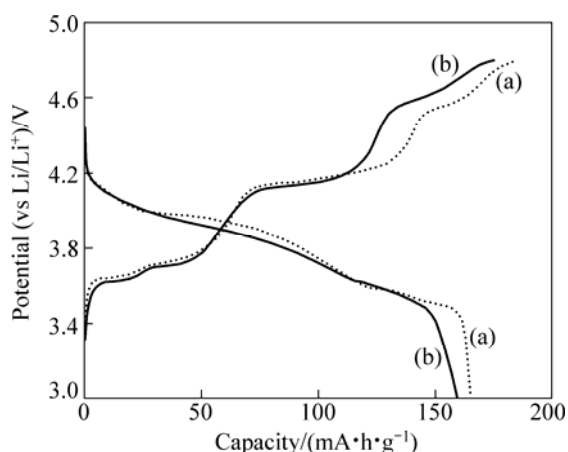


Fig.4 Second cycle charge/discharge curves of $\text{Li}_3\text{V}_2(\text{PO}_4)_3/\text{C}$ (a) and $\text{Li}_3\text{V}_{1.94}\text{Mn}_{0.09}(\text{PO}_4)_3/\text{C}$ (b)

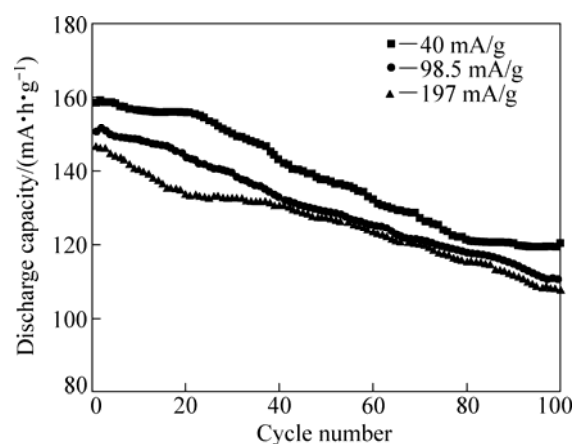


Fig.6 Discharge capacity vs cycle number for $\text{Li}_3\text{V}_{1.94}\text{Mn}_{0.09}(\text{PO}_4)_3/\text{C}$ at different current densities

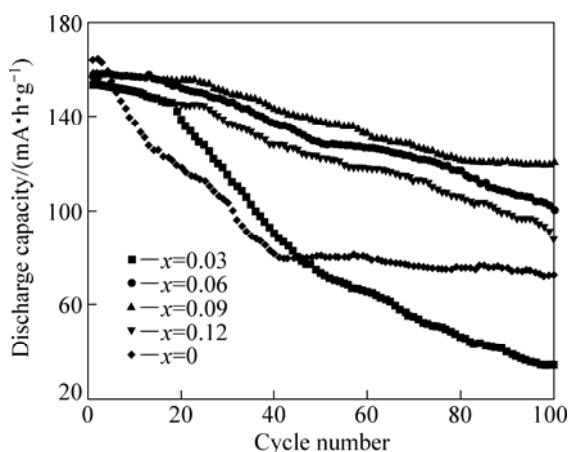


Fig.5 Cycling performance of $\text{Li}_3\text{V}_{2-2/3x}\text{Mn}_x(\text{PO}_4)_3/\text{C}$ ($x=0, 0.03, 0.06, 0.09, 0.12$)

improved. For example, after 100 cycles, the discharge capacity of $\text{Li}_3\text{V}_{1.94}\text{Mn}_{0.09}(\text{PO}_4)_3/\text{C}$ declines from initial $158.8 \text{ mA}\cdot\text{h}/\text{g}$ to $120.5 \text{ mA}\cdot\text{h}/\text{g}$ with a capacity retention of 75.9%; however, the discharge capacity of undoped one declines from initial $164.2 \text{ mA}\cdot\text{h}/\text{g}$ to $72.6 \text{ mA}\cdot\text{h}/\text{g}$ with a capacity retention of 44.2%.

Rate performance of the $\text{Li}_3\text{V}_{1.94}\text{Mn}_{0.09}(\text{PO}_4)_3/\text{C}$ is shown in Fig.6. The discharge capacity decreases with increasing the cycle number at different current densities, but the change is not sharp. At different current densities of $0.2C$, $0.5C$ and $1C$, the initial discharge capacities reach 158.8 , 150.8 and $146.4 \text{ mA}\cdot\text{h}/\text{g}$, respectively, and the discharge capacities maintain 120.4 , 110.6 and $107.5 \text{ mA}\cdot\text{h}/\text{g}$ after 100 cycles, respectively. From above data, we believe that the Mn-doping greatly improves the rate performance.

3.3 EIS analysis

Fig.7 shows typical Nyquist plots of the $\text{Li}_3\text{V}_2(\text{PO}_4)_3/\text{C}$ and $\text{Li}_3\text{V}_{1.94}\text{Mn}_{0.09}(\text{PO}_4)_3/\text{C}$ samples. Prior

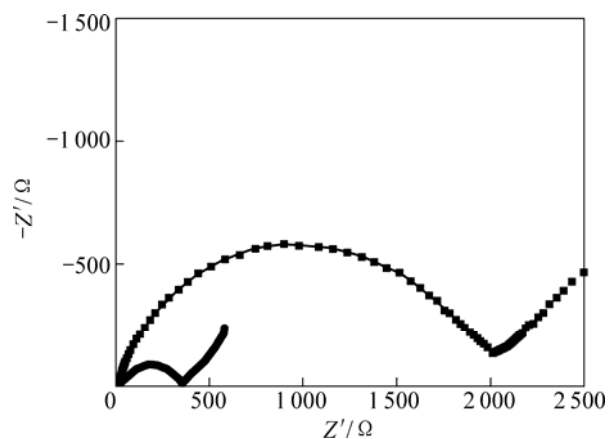


Fig.7 EIS of $\text{Li}_3\text{V}_2(\text{PO}_4)_3/\text{C}$ and $\text{Li}_3\text{V}_{1.94}\text{Mn}_{0.09}(\text{PO}_4)_3/\text{C}$

to the EIS measurement, the electrodes are cycled galvanostatically for 20 cycles between 3.0 and 4.8 V to ensure the stable formation of the SEI films on the surface of the electroactive particles. The EIS was then measured in the fully discharged state. As shown in Fig.7, the Nyquist plots are composed of a small intercept at high frequency, a semi-circle at high to medium frequency and a straight line at low frequency. The small intercept is almost the same ($14\text{--}16 \Omega$) for two samples, which represents the solution resistance. The semi-circle corresponds to the charge transfer resistance and double-layer capacitance. The sloping line corresponds to the diffusion of Li^+ ions in the electrode bulk, namely the Warburg impedance. It can be seen that the charge-transfer resistance on $\text{Li}_3\text{V}_{1.94}\text{Mn}_{0.09}(\text{PO}_4)_3/\text{C}$ electrode is much less than that on the undoped $\text{Li}_3\text{V}_2(\text{PO}_4)_3/\text{C}$. This result is similar to those previous reports[19]. The decrease of charge transfer indicates that the Mn-doping significantly can facilitate the kinetic process of electrochemical reaction on $\text{Li}_3\text{V}_{1.94}\text{Mn}_{0.09}(\text{PO}_4)_3/\text{C}$ electrode. This is favorable to

overcome kinetic limit in the course of charge/discharge, enhance the depth of extraction/insertion of Li^+ in active particles, reduce the difference of concentration of Li^+ which lies on surface and inner of active particles, and avoid the fade of capacity because the distortion of inner crystal structure of active particles happens[20].

4 Conclusions

1) The various Mn^{2+} -doped $\text{Li}_3\text{V}_{2-2/3x}\text{Mn}_x(\text{PO}_4)_3/\text{C}$ ($x=0, 0.03, 0.06, 0.09, 0.12$) cathode materials were synthesized by sol-gel method.

2) XRD diffraction results show that a monoclinic phase is obtained, and according to XPS analysis, the valences of V and Mn in $\text{Li}_3\text{V}_{1.94}\text{Mn}_{0.09}(\text{PO}_4)_3/\text{C}$ are +3, +2, respectively. Citrate is decomposed into carbon during calcination, and residual carbon exists in $\text{Li}_3\text{V}_{1.94}\text{Mn}_{0.09}(\text{PO}_4)_3/\text{C}$.

3) Electrochemical tests indicate that the Mn-doping into $\text{Li}_3\text{V}_2(\text{PO}_4)_3/\text{C}$ not only presents a tendency from multiphase reaction to single-phase reaction in the charge-discharge processes, but also reduces the charge transfer resistance. As a result, the cyclic stability and rate performance of $\text{Li}_3\text{V}_{2-2/3x}\text{Mn}_x(\text{PO}_4)_3/\text{C}$ cathode material can be effectively improved. Mn-doping is very effective for the improvement of the electrochemical performances of $\text{Li}_3\text{V}_2(\text{PO}_4)_3/\text{C}$.

References

- [1] PADHI A K, NAJUNDASWAMY K S, GOODENOUGH J B. Phospho-olivines as positive electrode materials for rechargeable lithium batteries [J]. *J Electrochem Soc*, 1997, 144(4): 1188–1194.
- [2] ZHONG Sheng-kui, YIN Zhou-lan, WANG Zhi-xing, GUO Hua-jun, LI Xin-hai. Synthesis and characterization of novel cathode material $\text{Li}_3\text{V}_2(\text{PO}_4)_3$ by carbon-thermal reduction method [J]. *Transactions of Nonferrous Metals Society of China*, 2006, 16(S1): S708–S710.
- [3] SAIDI M Y, BARKER J, HUANG H, SWOYER J L, ADAMSON G. Performance characteristics of lithium vanadium phosphate as a cathode material for lithium-ion batteries [J]. *J Power Sources*, 2003, 119–121: 266–272.
- [4] LI Y Z, ZHOU Z, REN M M, GAO X P, YAN J. Improved electrochemical Li insertion performances of $\text{Li}_3\text{V}_2(\text{PO}_4)_3$ /carbon composite materials prepared by a sol-gel route [J]. *Materials Letters*, 2007, 61: 4562–4564.
- [5] TANG A P, WANG X Y, LIU Z M. Electrochemical behavior of $\text{Li}_3\text{V}_2(\text{PO}_4)_3/\text{C}$ composite cathode material for lithium-ion batteries [J]. *Materials Letters*, 2008, 62: 1646–1648.
- [6] LI Y Z, ZHOU Z, GAO X P, YAN J. A promising sol-gel route based on citric acid to synthesize $\text{Li}_3\text{V}_2(\text{PO}_4)_3$ /carbon composite material for lithium ion batteries [J]. *Electrochim Acta*, 2007, 52: 4922–4926.
- [7] LI Y Z, ZHOU Z, REN M M, GAO X P, YAN J. Electrochemical performance of nano-crystalline $\text{Li}_3\text{V}_2(\text{PO}_4)_3$ /carbon composite material synthesized by a novel sol-gel method [J]. *Electrochim Acta*, 2006, 51: 6498–6502.
- [8] CHEN Q Q, WANG J W, TANG Z, HE W C, SHAO H B, ZHANG J Q. Electrochemical performance of the carbon coated $\text{Li}_3\text{V}_2(\text{PO}_4)_3$ cathode material synthesized by a sol-gel method [J]. *Electrochim Acta*, 2007, 52: 5251–5257.
- [9] CHANG C X, XIANG J F, SHI X X, HAN X X, YUAN L J, SUN J T. Rheological phase reaction synthesis and electrochemical performance of $\text{Li}_3\text{V}_2(\text{PO}_4)_3$ /carbon cathode for lithium ion batteries [J]. *Electrochim Acta*, 2008, 53: 2232–2237.
- [10] FU P, ZHAO Y M, DONG Y Z, AN X N, SHEN G P. Synthesis of $\text{Li}_3\text{V}_2(\text{PO}_4)_3$ with high performance by optimized solid-state synthesis routine [J]. *J Power Source*, 2006, 162: 651–657.
- [11] FU P, ZHAO Y M, AN X N, DONG Y Z, HOU X M. Structure and electrochemical properties of nanocarbon-coated $\text{Li}_3\text{V}_2(\text{PO}_4)_3$ prepared by sol-gel method [J]. *Electrochim Acta*, 2007, 52: 5281–5285.
- [12] SATO M, OHKAWA H, YOSHIDA K, SAITO M, UEMATSU K, TODA K. Enhancement of discharge capacity of $\text{Li}_3\text{V}_2(\text{PO}_4)_3$ by stabilizing the orthorhombic phase at room temperature [J]. *Solid-State Ionics*, 2000, 135: 137–142.
- [13] ZHONG Sheng-kui, LIU Le-tong, JIANG Ji-qiong, LI Yan-wei, WANG Jian, LIU Jie-qun, LI Yan-hong. Preparation and electrochemical properties of Y-doped $\text{Li}_3\text{V}_2(\text{PO}_4)_3$ cathode materials for lithium batteries [J]. *Journal of Rare Earths*, 2009, 27(1): 134–137.
- [14] LIU Su-qin, LI Shi-cai, HUANG Ke-long, CHEN Zhao-hui. Effect of doping Ti^{4+} on the structure and performances of $\text{Li}_3\text{V}_2(\text{PO}_4)_3$ [J]. *Acta Phys Chim Sinica*, 2007, 23: 537–542.
- [15] REN M M, ZHOU Z, LI Y Z, GAO X P, YAN J. Preparation and electrochemical studies of Fe-doped $\text{Li}_3\text{V}_2(\text{PO}_4)_3$ cathode materials for lithium-ion batteries [J]. *J Power Sources*, 2006, 162: 1357–1362.
- [16] SAIDI M Y, BARKER J, HUANG H, SWOYER J L, ADAMSON G. Electrochemical properties of lithium vanadium phosphate as a cathode material for lithium-ion batteries [J]. *Electrochim Solid State Lett A*, 2002, 5: 149–151.
- [17] OKU M, HIROKAWA K, IKEDA S. X-ray photoelectron spectroscopy of manganese-oxygen systems [J]. *Electron Spectroscopy and Related Phenomena*, 1975, 7: 465–473.
- [18] PISTOIA G, ANTONINI A, ROSATI R, BELLITTO C. Effect of partial Ga^{3+} substitution for Mn^{3+} in LiMn_2O_4 on its behaviour as a cathode for Li cells [J]. *Electroanalytical Chemistry*, 1996, 410: 115–118.
- [19] MI C H, ZHANG X G, ZHAO X B, LI H L. Synthesis and performance of $\text{LiMn}_{0.6}\text{Fe}_{0.4}\text{PO}_4$ /nano-carbon webs composite cathode [J]. *Materials Science and Engineering B*, 2006, 129: 8–13.
- [20] YANG S T, LIU Y X, YIN Y H, WANG H, WANG T. Effects of Ta ion doping on the physical and electrochemical performance of LiFePO_4/C [J]. *Chinese Journal of Inorganic Chemistry*, 2007, 23: 1165–1168.

锰掺杂对锂离子电池正极材料 $\text{Li}_3\text{V}_2(\text{PO}_4)_3/\text{C}$ 性能的影响

翟 静¹, 赵敏寿^{1,2}, 王丹丹¹

1. 燕山大学 环境与化学工程学院, 秦皇岛 066004;
2. 燕山大学 亚稳材料制备技术与科学国家重点实验室, 秦皇岛 066004

摘 要: 采用溶胶-凝胶法合成 $\text{Li}_3\text{V}_{2-2/3x}\text{Mn}_x(\text{PO}_4)_3$ ($0 \leq x \leq 0.12$)。采用 XRD、SEM、XPS、恒流充放电和电化学阻抗谱(EIS)研究 Mn 掺杂对 $\text{Li}_3\text{V}_2(\text{PO}_4)_3/\text{C}$ 结构和电化学性能的影响。XRD 研究表明: 掺杂少量的 Mn^{2+} 不会影响材料的结构, 所有样品均具有单一相态的单斜结构($P2_1/n$ 空间群)。XPS 分析表明: 在 $\text{Li}_3\text{V}_{1.94}\text{Mn}_{0.09}(\text{PO}_4)_3/\text{C}$ 中, V 和 Mn 的化合价分别为+3 和+2, 原料中的柠檬酸在煅烧过程中分解成 C 而残留在 $\text{Li}_3\text{V}_{1.94}\text{Mn}_{0.09}(\text{PO}_4)_3/\text{C}$ 中。电化学测试表明: 掺杂 Mn 改善了电极材料的循环性能和倍率性能, 正极材料 $\text{Li}_3\text{V}_{1.94}\text{Mn}_{0.09}(\text{PO}_4)_3/\text{C}$ 表现出最好的循环稳定性和倍率性能。在 40 mA/g 的放电电流密度下, 循环 100 次后, $\text{Li}_3\text{V}_{1.94}\text{Mn}_{0.09}(\text{PO}_4)_3/\text{C}$ 的放电容量从 158.8 mA·h/g 衰减到 120.5 mA·h/g, 容量保持率为 75.9%, 而未掺杂样品的放电容量从 164.2 mA·h/g 衰减到 72.6 mA·h/g, 容量保持率为 44.2%。当放电电流密度增加到 1C 时, $\text{Li}_3\text{V}_{1.94}\text{Mn}_{0.09}(\text{PO}_4)_3/\text{C}$ 的初始放电容量仍能达到 146.4 mA·h/g, 循环 100 次后, 放电容量保持为 107.5 mA·h/g。EIS 测试表明, 掺杂适量的 Mn^{2+} 减小了电荷转移阻抗, 这有利于 Li^+ 的脱嵌。

关键词: 锂离子电池; 正极材料; $\text{Li}_3\text{V}_2(\text{PO}_4)_3$; 溶胶-凝胶; 掺杂

(Edited by YANG Hua)